Somatic Cancer Mutations in the SUV420H1 Protein Lysine Methyltransferase Modulate Its Catalytic Activity

Alexander Bröhm [1], Hany Elsawy [2], Philipp Rathert [1], Srikanth Kudithipudi [1], Tabea Schoch [1], Maren Kirstin Schuhmacher [1], Sara Weirich [1] and Albert Jeltsch [1]

*1 - **Department of Biochemistry,** Institute of Biochemistry and Technical Biochemistry, Stuttgart University, Allmandring 31, 70569 Stuttgart, Germany*
*2 - **Department of Chemistry,** Faculty of Science, Tanta University, 31527 Tanta, El-Gharbia, Egypt*

***Correspondence to Albert Jeltsch:** Department of Biochemistry, Institute of Biochemistry and Technical Biochemistry, Allmandring 31, D-70569 Stuttgart, Germany. albert.jeltsch@ibtb.uni-stuttgart.de*
https://doi.org/10.1016/j.jmb.2019.06.021
Edited by Sepideh Khorasanizadeh

Abstract

SUV420H1 is a protein lysine methyltransferase that introduces di- and trimethylation of H4K20 and is frequently mutated in human cancers. We investigated the functional effects of eight somatic cancer mutations on SUV420H1 activity *in vitro* and in cells. One group of mutations (S255F, K258E, A269V) caused a reduction of the catalytic activity on peptide and nucleosome substrates. The mutated amino acids have putative roles in AdoMet binding and recognition of H4 residue D24. Group 2 mutations (E238V, D249N, E320K) caused a reduction of activity on peptide substrates, which was partially recovered when using nucleosomal substrates. The corresponding residues could have direct or indirect roles in peptide and AdoMet binding, but the effects of the mutations can be overcome by additional interactions between SUV420H1 and the nucleosome substrate. The third group of mutations (S283L, S304Y) showed enhanced activity with peptide substrates when compared with nucleosomal substrates, suggesting that these residues are involved in nucleosomal interaction or allosteric activation of SUV420H1 after nucleosome binding. Group 2 and 3 mutants highlight the role of nucleosomal contacts for SUV420H1 regulation in agreement with the high activity of this enzyme on nucleosomal substrates. Strikingly, seven of the somatic cancer mutations studied here led to a reduction of the catalytic activity of SUV420H1 in cells, suggesting that SUV420H1 activity might have a tumor suppressive function. This could be explained by the role of H4K20me2/3 in DNA repair, suggesting that loss or reduction of SUV420H1 activity could contribute to a mutator phenotype in cancer cells.

© 2019 Elsevier Ltd. All rights reserved.

Introduction

Histone posttranslational modifications such as acetylation, ubiquitination, phosphorylation and methylation play important roles in epigenetic signaling in combination with DNA methylation and other signals like histone variants and non-coding RNAs [1–4]. Histone posttranslational modifications influence the condensation of chromatin and regulate gene expression [5,6]. Moreover, they play an important role in many diseases including cancer [7,8]. Trimethylation of K20 of histone H4 (H4K20me3) is associated with constitutive heterochromatin, telomeres and centromeres, but it is also involved in gene silencing at euchromatic regions [9,10]. Methylation of histones mainly occurs on lysine and arginine residues. Lysine methylation is introduced by protein lysine methyltransferases (PKMTs) using *S*-adenosyl-L-methionine (AdoMet) as methyl group donor. Most histone modifying PKMTs belong to the SET (Su(var)3–9, enhancer-of-zeste and trithorax) domain family [11,12]. The SUV420H1 (KMT5B) and SUV420H2 (KMT5C) PKMTs introduce H4K20 methylation (H4K20me2/3) [13]. In addition, Smyd5 has been shown to deposit H4K20me3 in gene promoters of toll-like receptor 4 target genes in macrophages [14]. SUV420H1 and SUV420H2 prefer monomethylated

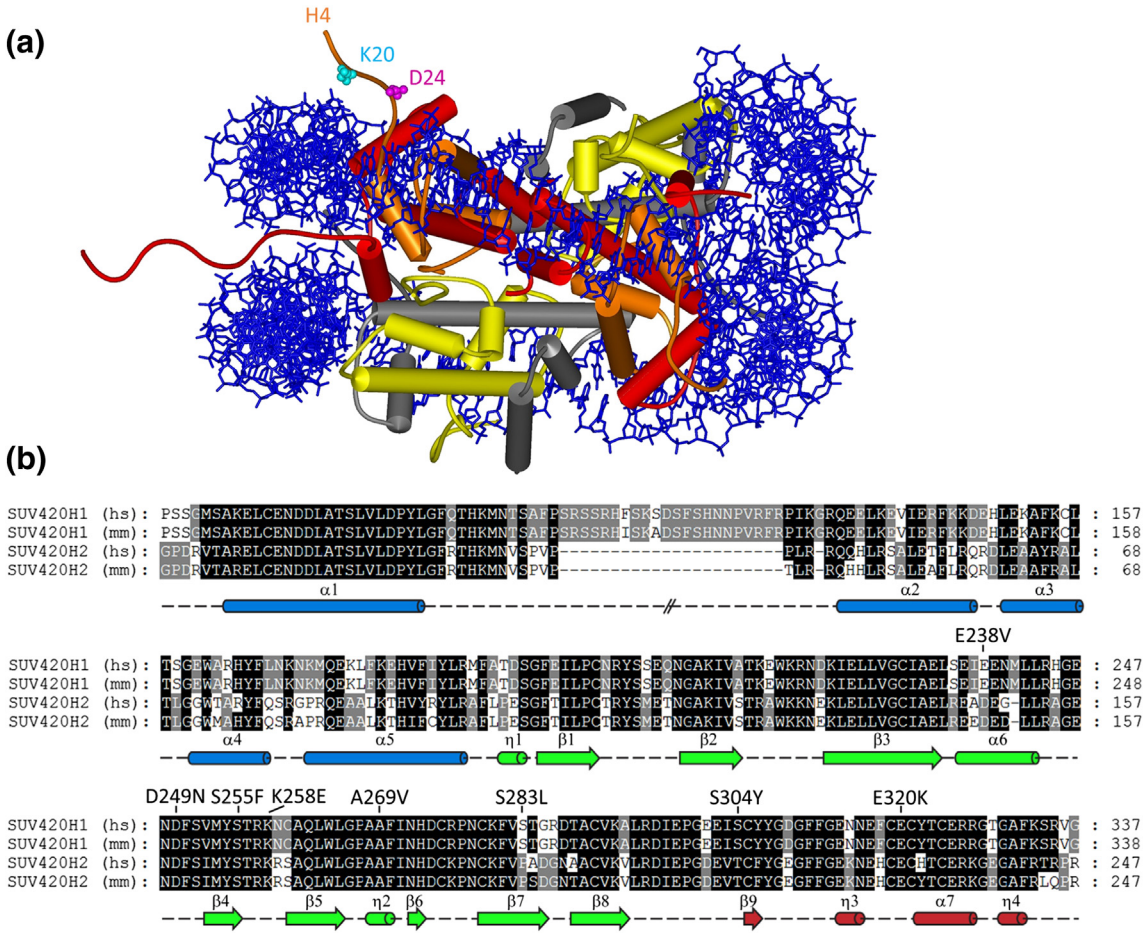

Fig. 1. Structure of the nucleosome substrate of SUV420H1 and sequence alignment of SUV420H enzymes. (A) Structure of the mononucleosome (PDB 1AOI) [19]. DNA is shown in blue, and the H3, H4, H2A and H2B histone proteins in red, orange, yellow and gray, respectively. K20 and D24 are shown on one H4 N-terminal tail. (B) Sequence alignment of the SET domains of human and mouse SUV420H1 and SUV420H2. Secondary structure elements are indicated as in Wu *et al.* [15]. Structural elements in the N-terminal part are colored blue, SET domain elements in green and post-SET elements in red. The amino acid mutations studied in this work are indicated.

H4K20me1 as substrate *in vitro* [15–17] and in cells [18], which is generated by the SET8 PKMT. The observation that a double knock-out of both SUV420H enzymes leads to an almost complete loss of H4K20me3 indicated that these enzymes introduce H4K20 methylation up to the trimethylation level in cells [13]. In agreement with the close proximity of the H4K20 position to the nucleosomal body and nucleosomal DNA (Fig. 1A), early studies already demonstrated that both SUV420H enzymes are more active on nucleosome substrates than on the free H4 protein or histone octamers, suggesting that they also contact the nucleosomal DNA [13].

The N-terminal catalytic SET domains of SUV420H1 and SUV420H2 share 65% amino acid sequence identity. They comprise an N-terminal helical domain (amino acid residues 63–191 of human SUV420H1), the core SET domain (191–303) and a post-SET domain (303–336) [15]. Both structures are very similar, and the SET and post-SET domains also share high similarity with other SET domain PKMTs [15,16]. For a more detailed description of the structure, we use a numbering of secondary structure elements based on the standard assignment of secondary structure elements in SET domain proteins (Fig. 1B) [15]. The N-terminal domain of SUV420H1 consists of a bundle of five helices (α1–α5). The SET domain is folded into four small antiparallel β-sheets, sheet 1 (ß1, ß2), sheet 2 (C-terminal part of ß3, ß4, ß5), sheet 3 (ß7, ß8 and the N-terminal part of ß3), sheet 4 (ß6, ß9) and one helix (α6). It forms a knot-like structure in which the carboxyl terminus is thread through a loop connecting ß6 and ß7. The Zn-binding post-SET domain mainly folds into three short helical segments (η3, α7, η4). The structure of SUV420H2 was also solved in complex with the substrate peptide [16], and it was found to be very similar to the structure of SUV420H1

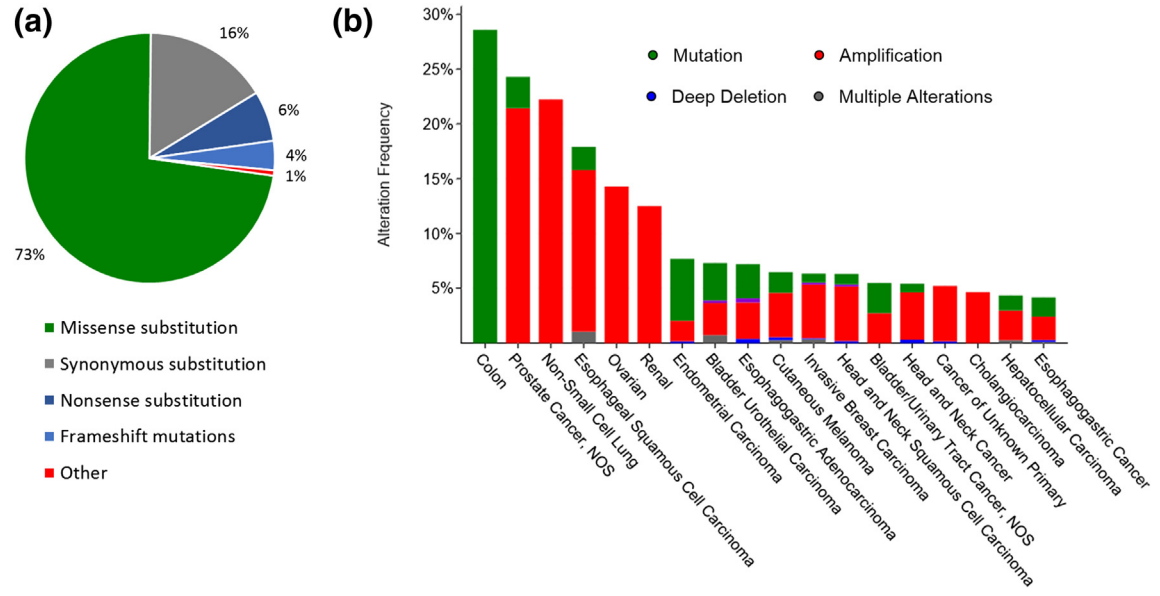

Fig. 2. D Distribution and types of somatics cancer mutations in SUV420H1. (A) Distribution of SUV420H1 mutation types listed in COSMIC. (B) Cancer types and types of SUV420H1 mutations based on all available data in cBioportal (233 studies, 71,554 samples, 69,715 patients). All data were retrieved in December 2018.

[15,16]. In biochemical assays, the substrate interaction of SUV420H1 was investigated, showing that it recognizes an (RY)-Kme1-(IVLM)-(LFI)-X-D peptide sequence, with strong readout at R19, V21, L22 and D24. Weaker readout was observed at R17 and H18 [17].

SUV420H1 and SUV420H2 are targeted to chromatin in an H3K9me3 and HP1 (heterochromatin-protein 1) dependent pathway [13]. In addition, heterochromatic targeting of SUV420H1 is mediated by interaction with RB1 (retinoblastoma-associated protein 1) [20]. Both SUV420H enzymes are differentially expressed, SUV420H1 expression is ubiquitous during embryogenesis and in all adult tissues, whereas SUV420H2 expression is mainly restricted to some adult tissues [21]. SUV420H1-introduced H4K20 methylation is bound by 53BP1 (p53-binding protein 1) and mediates DNA damage and p53 signaling during double-strand break repair [22–24]. An inhibitor of the SUV420H enzymes has been shown to reduce 53BP1 foci formation after DNA damage [25]. Moreover, SUV420H1-generated H4K20 methylation stimulates non-homologous end joining (NHEJ)-directed DNA repair [25,26]. Both SUV420H enzymes are involved in regulating the expression of target genes, for example, in myogenesis [27] and ε-globin expression [28]. SUV420H1 together with the MYST2 histone acetyltransferase is part of the BRD1 (bromodomain-containing protein 1) interaction network that has a direct impact on mental disorder risk [29]. Moreover, SUV420H1 was shown to interact with the glucocorticoid receptor (GR) and influence GR target gene expression [30].

SUV420H1 has several well-documented disease connections (Fig. 2). It was shown to be a key candidate gene in neurodevelopmental and neuropsychiatric disorders [31], and genetic evidence suggests that heterozygous loss-of-function mutations in SUV420H1 cause one form of autosomal dominant mental retardation, which is characterized by significantly impaired general intellectual abilities and adaptive behavior and manifests during the developmental period (MRD51, OMIM 61778, Uniprot diseases DI-05152). In addition, SUV420H1 has been directly connected to cancer because loss of histone H4K20 trimethylation is correlated with poor prognosis and increased invasive activity in breast cancer [32]. SUV420H1 has been found to enhance the phosphorylation and transcription of ERK1 (extracellular-signal-regulated kinase 1) in cancer cells [33]. It was proposed that this effect is mediated by ERK1 methylation by SUV420H1 [33], but this finding could not be validated [17].

Like other chromatin modifiers, SUV420H1 is often mutated in cancer cells [8,34,35]. A recent analysis of COSMIC mutational data revealed that SUV420H1 has the seventh highest fraction of somatic tumor mutations among all PKMTs when compared to the size of the protein [36]. This finding motivated us to investigate the functional effects of somatic cancer mutations in this enzyme. We selected eight mutations based on the 3D structure of SUV420H1 and investigated their consequences on the H4K20 methylation activity of the enzyme using peptide and nucleosome substrates. Mechanistically, our data provide evidence for the role of nucleosomal contacts in the regulation of SUV420H1, and they support the

central importance of the contact between H4 D24 and SUV420H1 K258. Seven of the cancer mutations studied here led to a reduction in the catalytic activity of SUV420H1, suggesting that SUV420H1 might function as a tumor suppressor gene, perhaps through its connection to DNA repair.

Materials and Methods

Cloning, protein expression and purification

The bacterial pDEST15 expression construct containing the GST-fused murine SUV420H1 (amino acid 1–383 of SwissProt entry Q3U8K7) [17] was used as template for the generation of the desired point mutants. Site-directed mutagenesis was conducted by the PCR megaprimer method as described [37]. The presence of the point mutations was confirmed by Sanger sequencing. The pEYFP full-length human SUV420H1 fusion construct was received as a kind gift of G. Schotta [13]. Site-directed mutagenesis was applied to introduce the same point mutations as for the murine SUV420H1 construct. The wild-type and mutant constructs were sub-cloned into the RT3GEPIR plasmid backbone containing the doxycycline-inducible TRE3G promotor and the rtTA3 repressor to enable regulated expression upon dox treatment [38].

For protein expression, *Esherichia coli* BL21 (DE3) codon plus cells (Agilent) were transformed with the bacterial expression constructs by the heat shock method and were grown in Luria–Bertani medium at 37 °C to an OD_{600} of 0.6–0.8. Expression of the proteins was induced overnight with 1 mM IPTG at 20 °C. The cells were harvested by centrifugation at 4200 *g*. For purification, the cell pellet was resuspended in sonication buffer [20 mM Hepes (pH 8), 500 mM KCl, 1 mM EDTA, 2 mM DTT, 10% glycerol) and lysed by sonication. The lysate was cleared by centrifugation at 45,000 *g* for 1 h and passed through a 0.45-µm syringe filter with glass fiber prefilter. An NGC quest plus FPLC system (Bio-Rad) was used to equilibrate a 1-ml column filled with glutathione agarose 4B beads (Macherey-Nagel) with sonication buffer. The lysate was passed through the column, and weakly bound proteins were removed by washing with 30 column volumes of sonication buffer. The protein was eluted from the column with sonication buffer containing 40 mM reduced glutathione. Fractions were pooled according to highest protein concentration and dialyzed against low glycerol dialysis buffer [20 mM Hepes (pH 8), 200 mM KCl, 2 mM DTT, 10% glycerol] for 3 h. Thereafter, the sample was dialyzed against high glycerol dialysis buffer [20 mM Hepes (pH 8), 200 mM KCl, 2 mM DTT, 60% glycerol] overnight and stored at −20 °C.

Circular dichroism spectroscopy

Folding of the purified proteins was analyzed by circular dichroism (CD) spectroscopy using a J-815 CD spectrophotometer (JASCO Corporation, Tokyo, Japan) in buffer containing 200 mM KCl, 10 mM Hepes (pH 7.5) and 5% glycerol at protein concentrations of 10 µM. The spectra were collected at 20 °C using a 0.1-mm cuvette in a wavelength range between 190 and 250 nm using a scanning speed of 100 nm/min, bandwidth of 1 nm and data integration time of 1 s. For each sample, 30 scans were collected and averaged.

Native mononucleosome isolation

Native mononucleosomes were prepared from mouse embryonic fibroblast (MEF) cells basically as described [39]. Briefly, MEF cells were lysed with NP-40 buffer [10 mM Tris–HCl (pH 7.4), 2 mM $MgCl_2$, 500 µM PMSF, 0.6% NP-40], and the extracted nuclei were digested with micrococcal nuclease (MNase) for 5 min in the presence of 1 mM $CaCl_2$. The digestion was stopped by addition of 2 mM EGTA, and the mononucleosomes were isolated from the nuclei by treatment with 0.1% Triton X-100 and 300 mM NaCl. Sufficient chromatin digestion was confirmed by gel electrophoresis. Finally, the nucleosomes were flash frozen in liquid N_2 and stored at −80 °C.

Reconstitution of recombinant nucleosomes

Recombinant histone proteins were isolated from *E. coli* basically as described [40]. In brief, protein constructs were overexpressed as described above, resuspended in SAU 200 buffer [NaOAc/HCl (pH 7.5), 6 M urea, 1 mM EDTA pH 8, 5 mM β-mercaptoethanol, 200 mM NaCl], lysed by sonication and cleared as stated above. The cleared lysate was passed over an SP HP cation exchange column (GE Healthcare) equilibrated with SAU 200 buffer using the NGC quest plus FPLC system. The column was washed with 8 column volumes of SAU 200 buffer, and the bound protein was eluted with a salt gradient up to 800 mM NaCl. The gradient slope was adjusted for each individual histone protein. Fractions containing the desired protein were dialyzed against distilled water overnight, subsequently dried in a vacuum centrifuge and stored at 4 °C.

The reconstitution of histone octamers was carried out as described [41]. Briefly, the dried proteins were dissolved in unfolding buffer [7 M guanidinium HCl, 20 mM Tris–HCl (pH 7.5), 10 mM DTT], mixed in a molar ratio of 1 (H3, H4) to 1.2 (H2A, H2B) and dialyzed against refolding buffer [2 M NaCl, 10 mM Tris–HCl (pH 7.5), 1 mM EDTA pH 8, 5 mM β-mercaptoethanol] overnight. Afterward the sample was passed through a Superdex 200 PG size

exclusion column (GE Healthcare) equilibrated with refolding buffer to isolate the fully assembled histone octamers. Fractions containing pure octamers were concentrated using spin filters (Amicon, Merck), shock frozen in liquid N_2 and stored at −80 °C.

The DNA fragment required for the assembly of nucleosomes was based on the Widom 601 positioning sequence [42] to which a CG-rich linker DNA fragment was added by PCR amplification. The resulting 240-bp fragment was amplified by large scale PCR reactions. For the nucleosome assembly, DNA was mixed with histone octamers in a twofold molar excess and dialyzed against RB buffer [10 mM Tris–HCl (pH 7.5), 1 mM EDTA pH 8] containing 2 M NaCl, which was continuously replaced by RB buffer containing 250 mM NaCl over the time course of 24 h. Afterward the samples were concentrated using spin filters, flash frozen in liquid N_2 and stored at −80 °C.

Methylation assays

For *in vitro* methylation experiments, 2 µM enzyme was incubated in methylation buffer [20 mM Hepes (pH 8), 50 mM NaCl, 5 mM DTT] containing 0.76 µM radioactively (^{3}H)-labeled AdoMet (PerkinElmer) and substrate [1.8 µM H4 peptide residues 12–29, 1.8 µM native mononucleosomes, 350 nM recombinant H4 (NEB), or 80 nM recombinant nucleosomes] for 4 h at 20 °C. The reaction was stopped by addition of SDS loading buffer and incubation at 95 °C for 5 min. Tricine SDS-PAGE was used to resolve the desired bands after peptide methylation reactions, while standard 16% SDS-PAGE was employed for nucleosome and H4 methylation experiments. The gels were incubated for 1 h in Amplify solution (GE Healthcare) and dried at 60 °C in vacuum. The dried gels were imaged using photosensitive ECL hyperfilm (GE Healthcare) at −80 °C in the dark.

Pull-down experiments

Streptavidin beads were washed three times with interaction buffer [25 mM Tris–HCl (pH 7.5), 100 mM KCl, 5 mM $MgCl_2$, 10% glycerol, 0.1% NP-40, 0.2 mM PMSF]. H4K20me1 peptide (0.2 µM) and SUV420H1 enzyme (0.1 µM) were mixed in 200 µl interaction buffer and incubated with the beads under constant rotation for 2 h at 8 °C. One identical sample without peptide was used as a control for nonspecific binding. Subsequently, the beads were washed three times with interaction buffer containing 300 mM KCl and once with interaction buffer. The supernatant was removed, and the beads were heated to 95 °C for 10 min in 30 µl SDS-gel loading buffer. The samples were resolved by 12% SDS-PAGE and analyzed by Western blot using a GST antibody (GE Healthcare, 27457701A) and ECL substrate (Thermo Fisher).

Generation of stable cell lines and analysis of methylation state

SUV420H1 and SUV420H2 double knock-out (dko) murine embryonic fibroblast (MEF) cells were a kind gift of G. Schotta [43]. MEF cells were cultured in DMEM media supplemented with 10% fetal bovine serum, 2 mM L-glutamine, 1× penicillin/streptomycin, 1 mM sodium pyruvate, 1× non-essential amino acid solution and 0.1 mM β-mercaptoethanol. For the stable integration of the SUV420H1 gene into the MEF dko cells, PlatE packaging cells were transfected with the respective retroviral transduction construct and the Gag Pol helper plasmid by calcium phosphate co-precipitation. After 48 h, the medium containing the recombinant ecotropic retrovirus particles was passed through a 0.45-µm syringe filter and added to the MEF dko cells at 70% confluence. This infection was repeated up to three times. After 48 h, selection was performed by treatment of the cells with 3 µg/ml puromycin over 5 days. Expression of the introduced gene was induced by addition of 1 µg/ml doxycycline for 4 days. The induction efficiency was evaluated by flow cytometry (MACSQuant VYB, Miltenyi Biotec). The cells were harvested, flash frozen in liquid nitrogen and stored at −80 °C. Histone proteins were isolated from MEF cells by acid extraction as described [44]. The samples were separated by SDS-PAGE and analyzed by Western blot using an H4K20me3 antibody (Abcam, ab9053) and SuperSignal Femto ECL substrate (Thermo Fisher). The same blot was probed with a H3 antibody (Abcam, ab1791) as loading control. H4K20me1 methylation was analyzed using a H4K20me1 antibody (Active motif, 39175).

Results

Selection of SUV420H1 mutations

PKMTs are frequently mutated in human cancers, but the functional consequences of these mutations are not known in most cases [8,34,35]. We collected information about mutations of SUV420H1 in cancer tissues from the COSMIC [45] and cBioportal [46,47] databases. The distribution of mutations showed an enrichment of gene amplifications and missense mutations with low frequencies of clear loss-of-function mutations like deletions, frameshifts or non-sense mutations (Fig. 2A and B). Analysis of cBioportal revealed that genetic alterations in SUV420H1 are very prominent in several cancers including colon, prostate, lung, esophagus, ovarian and renal tumors (Fig. 2B). COSMIC reports overexpression of SUV420H1 in several cancers including esophagus (18%), upper aerodigestive

Table 1. Compilation of mutational data regarding the residues investigated in this study

Residue	Mutation	cBioportal
E238	E238V	Lung adenocarcinoma (taken from COSMIC)
D249	D249N	Rectal adenocarcinoma, 4 cases
	D249H	Prostate adenocarcinoma
	D249G	Breast invasive ductal carcinoma
S255	S255F	Breast carcinoma, 4 cases
	S255Y	Hepatocellular carcinoma (taken from COSMIC)
K258	K258E	Uterine endometriod carcinoma, 3 cases
A269	A269V	Uterine endometriod carcinoma, 3 cases
S283	S283L	Lung adenocarcinoma, 2 cases
S304	S304Y	Mucinous adenocarcinoma of the colon and rectum
E320	E320K	Adenocarcinoma (colon, rectum)

The table is based on all available data in cBioportal (233 studies, 71,554 samples, 69,715 patients) and COSMIC (all retrieved in Dec, 2018).

tracts (14%), stomach (12%), breast or lung (both 11%). Focusing mainly on recurrent missense mutations, we screened the mutated residues for putative functional roles and selected eight mutations for further analysis: E238V, D249N, S255F, K258E, A269V, S283L, S304Y and E320K (Table 1). All residues are fully conserved in human and mouse SUV420H1, and most of them are identical between SUV420H1 and SUV420H2 (Fig. 1B).

Mutagenesis, expression and purification of SUV420H1 mutants

To study the effect of the cancer mutations in SUV420H1, they were introduced by site-directed mutagenesis into a bacterial GST-tagged SET domain expression construct for murine SUV420H1 [17]. The wild-type and mutant proteins were overexpressed in *E. coli* and purified by affinity

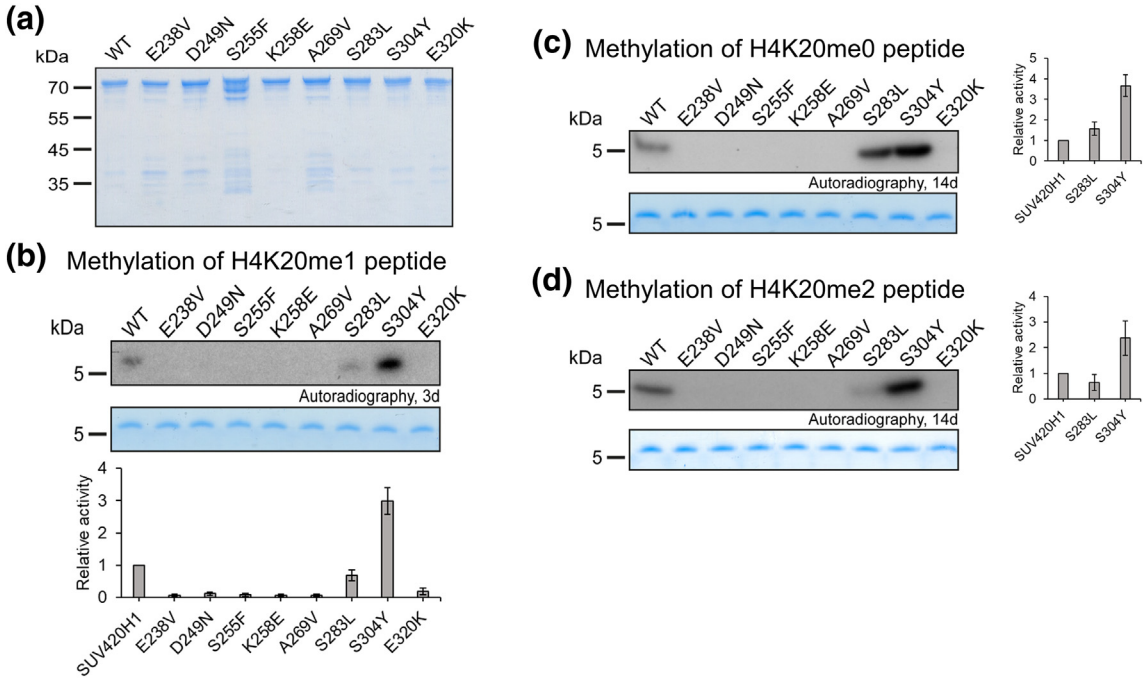

Fig. 3. Protein expression and catalytic activity of SUV420H1 mutants. (A) Example of the purified proteins used in this study. The image shows an SDS gel stained with Coomassie BB. (B) Catalytic activity of the wild-type and mutant SUV420H1 proteins using an H4 (12–29) peptide containing K20me1 as substrate. The peptide was incubated with SUV420H1 proteins in the presence of radioactively labeled AdoMet. The image shows an autoradiogram of a Tricine SDS-gel. The lower panel displays a Coomassie BB-stained gel showing the equal H4 peptide input of the methylation reactions. (C) Catalytic activity of the wild-type and mutant SUV420H1 proteins using an H4 (12–29) peptide containing K20me0. (D) Catalytic activity of the wild-type and mutant SUV420H1 proteins using an H4 (12–29) peptide containing K20me2. The exposure times of the films are indicated. The quantification of the data is based on five (panel B) or four (panels C and D) repetitions; the error bars display the SD.

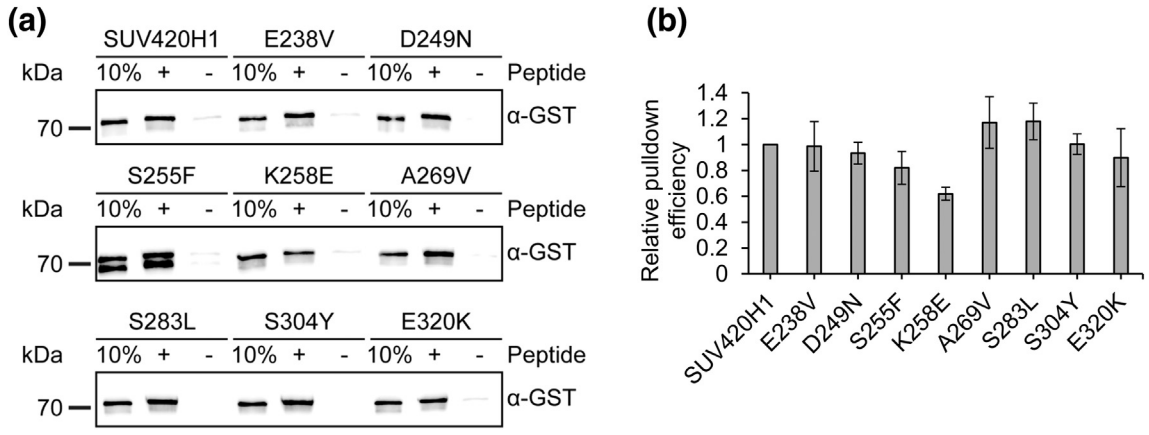

Fig. 4. Peptide pull-down experiments. (A) Western blot after pull-down of SUV420H1 enzymes with biotin-tagged H4K20me1 peptide. The peptide was incubated with the SUV420H1 enzymes and bound to streptavidin beads. The image shows 10% of the input material as loading control, the pulled protein as well as a mock pull-down without peptide. (B) Quantification of the data in panel A based on two to four repetitions; the error bars represent the SD. K258E showed a significant reduction in peptide interaction; all other fluctuations were not significant.

chromatography (Fig. 3A). The folding of the purified proteins was investigated by CD spectroscopy showing that all CD spectra were superimposable within the noise range in the wavelength region of 200–240 nm (Suppl. Fig. 1). While this finding does not exclude local structural differences, it confirmed comparable overall folding of all protein preparations.

Catalytic activity of SUV420H1 mutants on H4 peptide substrates

For an initial test, the catalytic activity of wild-type SUV420H1 and its mutants was tested on H4 peptide substrates (H4 12–29). Initial experiments were conducted with monomethylated H4K20me1,

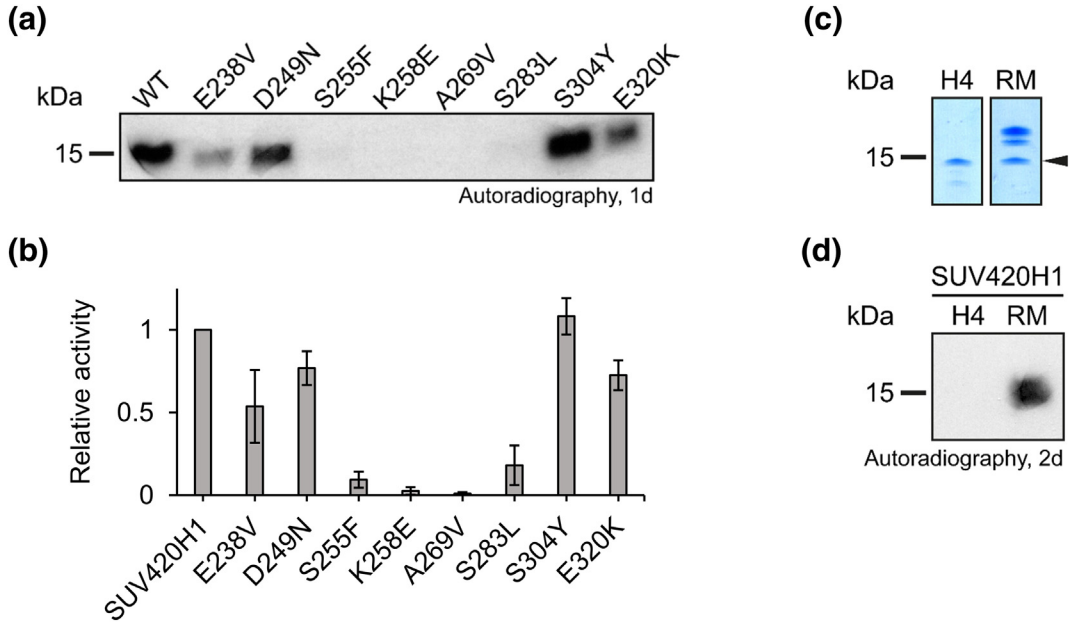

Fig. 5. *In vitro* nucleosome methylation activity of wild-type and mutant SUV420H1 proteins. (A) Native nucleosomes were isolated from SUV420H dko MEF cells (Suppl. Fig. 2) and used as substrate for an *in vitro* methylation analysis. The nucleosomes were incubated with SUV420H1 proteins in the presence of radioactively labeled AdoMet. The image shows an autoradiogram of an SDS-gel. (B) Quantification of the data shown in panel A based on three repetitions; the error bars display the SD. (C) Loading control of recombinant H4 protein (New England Biolabs) and recombinant mononucleosomes (RM) showing equal amounts of H4 protein. The image shows an SDS-gel stained with Coomassie BB. (D) Methylation activity of wild-type SUV420H1 on unmethylated H4 and recombinant mononucleosomes. The image shows an autoradiogram of an SDS-gel. The exposure times of the films are indicated.

which is the preferred peptide substrate of SUV420H1 *in vitro* and *in vivo*. The peptide was incubated with the SUV420H1 enzymes in the presence of radioactively labeled AdoMet. Afterward the samples were separated on a Tricine SDS-gel and the transfer of methyl groups to the peptide was detected by autoradiography (Fig. 3B). Our data revealed an increased activity of S304Y, slight reduction in activity of S283L and very low activities of all other mutants. Additional kinetics were conducted with the K20 unmethylated and dimethylated H4 peptide substrates (Fig. 3C and D). They confirmed a reduced activity with both substrates. After long exposition times, catalytic activities were detected with the wild-type enzyme, S283L and S304Y. In case of S304Y, the relative preference for H4K20me1 was not affected by the mutation. S283L showed increased activity with the H4K20me0 substrate compared to wild-type, while H4K20me1 and H4K20me2 were methylated by this mutant with a reduced relative rate, but this effect occurred at a very low overall activity level. In summary, these results revealed strong effects of six of the mutations on the ability of SUV420H1 to methylate peptide substrates (E238V, D249N, S255F, K258E, A269V and E320K), while one mutation led to a hyperactive enzyme (S304Y).

Binding affinity of SUV420H1 mutants to the native peptide substrate

To assess if the loss of activity of most mutants of the SUV420H1 methyltransferase could be attributed to reduced binding of the target peptide, we employed a pull-down assay with biotin-tagged H4K20me1 peptide and streptavidin beads. The pulled protein fraction was separated on an SDS-gel and detected by Western blot against GST. The data revealed a reduced pull-down efficiency of the K258E mutant in comparison with the SUV420H1 wild-type (Fig. 4A and B). Peptide pull-down of all other mutants was not significantly affected.

Catalytic activity of SUV420H1 mutants on nucleosomal substrates *in vitro* and in cells

Next we aimed to investigate the catalytic activity of SUV420H1 and its mutants on native nucleosomal substrates. For this experiment, nucleosomes were isolated from murine SUV420H1 and SUV420H2 dko MEF cells [43] (Suppl. Fig. 2A). These nucleosomes have strongly reduced H4K20me2/3 levels but instead show accumulation of H4K20 monomethylation (Suppl. Fig. 2B and C), which makes them good substrates for *in vitro* methylation

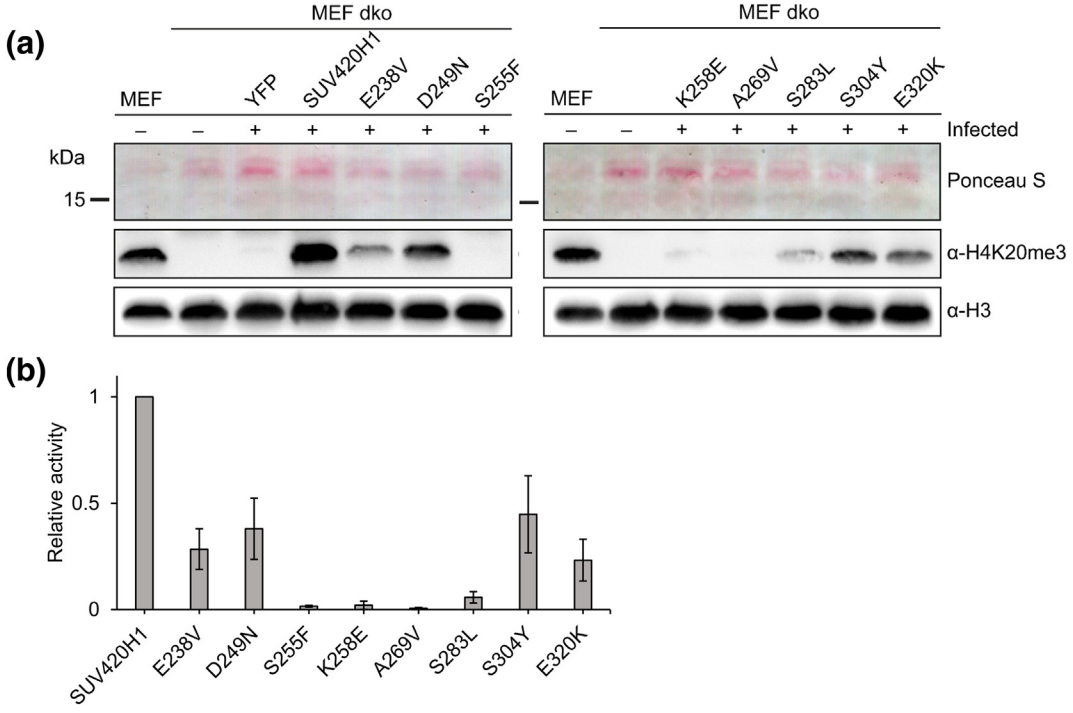

Fig. 6. Methylation activity of wild-type and mutant SUV420H1 proteins in cells. (A) SUV420H1 was expressed in SUV420H dko cells for 4 days (Suppl. Fig. 3). Then, histones were prepared and analyzed by Western blot using antibodies specific for H4K20me3 methylation and H3. (B) Quantification of the data shown in panel A based on three repetitions; the error bars display the SD.

reactions with SUV420H1. The isolated nucleosomes were incubated with the SUV420H1 wild-type and mutant enzymes in the presence of radioactively labeled AdoMet. Afterward, the samples were separated on an SDS gel, and the transfer of methyl groups to the H4 protein was detected by autoradiography (Fig. 5A). The data revealed a wild-type-like activity of S304Y; slightly reduced activities of E238V, D249N and E320K; and very low activity of all other mutants (S255F, K258E, A269V and S283L) (Fig. 5B). The relative high activities obtained with E238V, D249N and E320K were particularly striking because these mutants were almost inactive on peptide substrates. On the other hand, S283L was much less active on nucleosomal substrates than on peptide substrates.

In addition, the activity of the SUV420H1 wild-type on unmethylated recombinant H4 protein and unmethylated recombinant nucleosomes (Fig. 5C and D) was tested in the same assay as described above. No activity was observed on recombinant H4, which can be explained by the preference of SUV420H1 for substrates containing H4K20me1. However, the recombinant mononucleosomes were efficiently methylated by SUV420H1, although they contain the target lysine in the K20me0 state (Fig. 5D). This finding is in agreement with previous data showing that SUV420H1 is more active with nucleosomal substrates [13].

Catalytic activity of SUV420H1 mutants in cells

To test the activity of the SUV420H1 mutants in cells, we used the SUV420H dko MEF cells and prepared stable cell lines by viral transduction, which express EGFP fused wild-type or mutant SUV420H1 under the control of doxycycline. Four days after SUV420H1 induction, the expression of the target construct was analyzed by flow cytometry (Suppl. Fig. 3). Histones were extracted and their H4K20me3 content was determined by Western blot (Fig. 6). Despite relatively low expression levels, when compared with the YFP control, expression of wild-type SUV420H1 led to a strong increase in H4K20me3 in the MEF dko cells, reaching levels even slightly higher than in wild-type MEF cells. The E238V, D249N and S255F mutants showed similar expression levels as the wild-type construct, but moderately reduced (in the case of S255F strongly reduced) H4K20me3 levels. The K258E, A269V S283L and S304Y mutants showed reduced expression of around 60% of wild-type levels, and the expression of E320K was around 30% of wild-type. The K258E, A269V and S283L mutants showed very low H4K20me3 levels, indicating a strong reduction in specificity activity when compared with wild-type. S304Y and E320K also showed a reduction of H4K20me3, but in these cases, the relative expression of the constructs was similarly reduced.

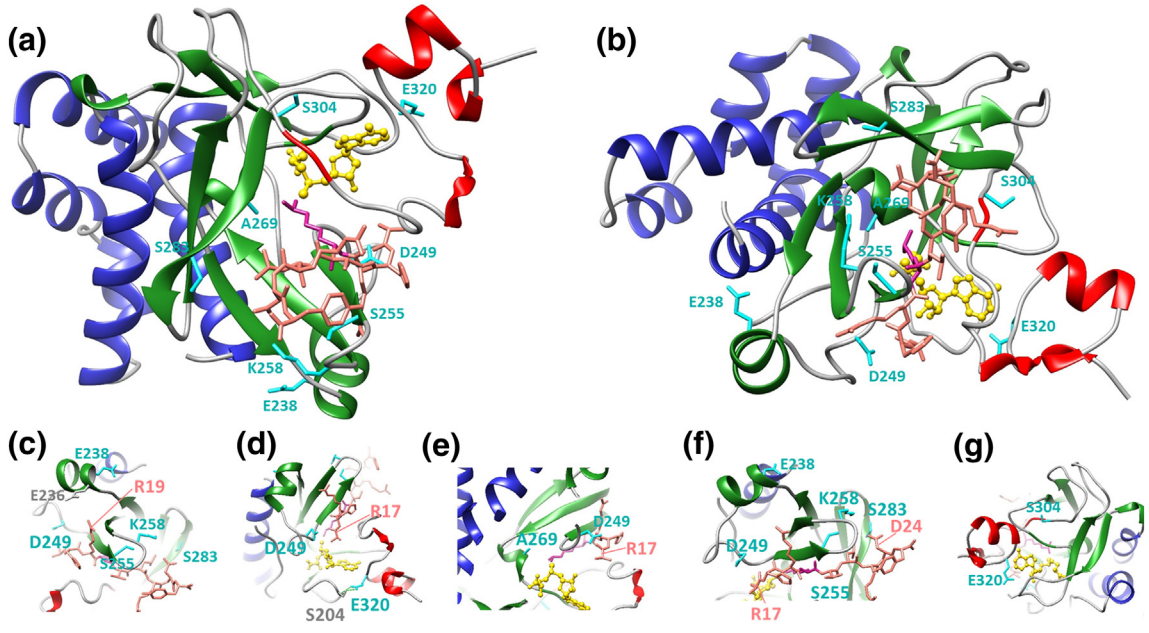

Fig. 7. Location of the cancer mutations in the structure of human SUV420H1. (A and B) Overview images of the structure of human SUV420H1 (PDB 3s8p) [15]. The protein is shown as gray ribbon with secondary structure elements colored as in Fig. 2B. AdoMet is shown in gold, and the residues mutated in this work are displayed in cyan. The H4 peptide (salmon, with K20 in pink) was taken from the structure of mouse SUV420H2 (PDB 4au7) [16] after superposition of both protein structures. The image is shown from two different viewpoints. (C–G) Additional images showing the different mutated residues and their neighbors in more details and from different viewpoints.

Table 2. Summary of the results of this study

Mutation	Category	Methylation activity on peptide substrate	Methylation activity on nucleosomal substrate	Methylation activity in cells
S255F	Group 1	Strongly reduced	Strongly reduced	Strongly reduced
K258E	Group 1	Strongly reduced (reduced binding)	Strongly reduced	Strongly reduced
A269V	Group 1	Strongly reduced	Strongly reduced	Strongly reduced
E238V	Group 2	Strongly reduced	Moderately reduced	Moderately reduced
D249N	Group 2	Strongly reduced	Moderately reduced	Moderately reduced
E320K	Group 2	Strongly reduced	Moderately reduced	n.d.
S283L	Group 3	About wild-type	Reduced	Strongly reduced
S304Y	Group 3	Hyperactive	About wild-type	n.d.

n.d., not determined.

Since it was not possible to increase the expression of these mutants in several attempts, we conclude that we cannot evaluate their cellular activity based on these data. In summary, the most severely reduced H4K20me3 levels were observed with S255F, K258E, A269V and S283L, which already showed the strongest reduction of *in vitro* activity using nucleosomal substrates.

Discussion

In this study, the effects of eight somatic mutations of the SUV420H1 PKMT, which have been identified in cancer patients, were investigated. To get more insight into the potential roles of these residues, we superimposed the available structures of human SUV420H1 AdoMet complexes (PDB 3s8p) [15] with the structure of mouse SUV420H2 containing the bound H4 peptide (PDB 4au7) [16] using DeepView SPDB viewer. The protein structures superimposed very well (RMSD 1.04 Å involving 216 Cα-atoms), indicating that the derived model of the SUV420H1–peptide interaction is meaningful. The resulting model (Fig. 7A and B) was inspected to derive potential roles of the affected amino acid residues:

E238 is located in α6 next to E236 at the N-terminus of this helix (Fig. 7C). E236 is putatively involved in the recognition of H4-R19, a very important peptide contact point of SUV420H1 [17]. E238 itself points toward α1 in the N-terminal subdomain, and by this, it may connect the peptide recognition with the rest of the domain.

D249 is in hydrogen bonding distance to H4-R17, and it might play a direct role in peptide recognition (Fig. 7C–E). In addition, it hydrogen bonds to G246, which forms a second H-bond to R17.

S255 is located at the end of ß-strand ß4 (Fig. 7F). It is directly involved in the stabilization of the loop containing K258.

K258 is placed at the turn connecting ß4 and ß5 (Fig. 7F). It directly points toward H4-D24, one of the most important contact points between SUV420H1 and the target peptide identified in our previous specificity analysis of SUV420H1 [17].

A269 is placed next to the active site pocket of SUV420H1 in a distance of about 3 Å to the bound AdoMet (Fig. 7E).

S283 is positioned in ß7 forming the pseudoknot structure (Fig. 7F). It anchors the C-terminal part of the SET domain, which is involved in peptide and AdoMet interaction. Modeling suggests that S283 might contribute a nucleosome contact.

S304 is located in front of ß9 at the basis of the pseudoknot structure (Fig. 7G).

E320 is located in the C-terminal helical part of SUV420H1 at the beginning of α7 (Fig. 7G). It hydrogen bonds to S204 and by this connects this part to the loop of the SET domain, which is directly involved in AdoMet binding.

The mutant enzymes were purified and their catalytic activity tested on peptide and nucleosomal substrates *in vitro* and in cells. Interestingly, all residues selected for our study showed striking effects on enzyme activity, which is supporting the hypothesis that their corresponding mutations have an active role in tumorigenesis. In detail, our study has revealed three types of responses to mutations of these important residues in SUV420H1 (Table 2).

Group 1 mutations led to a reduction of catalytic activity on peptide and nucleosome substrates (S255F, K258E, A269V). The effect of A269V can be explained by the position of this residue next to the active site and AdoMet binding site where the replacement of A by the larger V putatively causes structural rearrangements that disrupt enzymatic activity. K258 is putatively involved in the recognition of D24 in the H4 peptide. This contact is essential for SUV420H1 activity [17], and it would be disrupted by the exchange of K to E. It is noteworthy that the K258E exchange was the only mutation that led to reduced peptide binding in pull-down experiments, which further supports the central role of K258 in the H4 tail interaction. S255 could be indirectly involved in the contact of K258 to H4 D24, by positioning and stabilization of the loop containing K258.

Group 2 mutations caused reduction of activity on peptide substrates, but activity was partially recovered when using the nucleosomal substrate (E238V, D249N, E320K). The reduced activity of the mutants on the peptide substrate suggests that E238, D249 and E320 are directly or indirectly involved in peptide and AdoMet binding. However, based on our data, this functional impairment can be overcome by additional interactions between the enzyme and the nucleosome substrate. This finding is in agreement with the increased overall activity of SUV420H1 on nucleosomal substrates and it points toward the importance of nucleosomal contacts for controlling the activity of SUV420H1.

Group 3 mutations caused the opposite effect as group 2 because they showed higher activity with peptide substrates than with nucleosomal substrates. In the case of S283L, this result can be interpreted because modeling suggests that this residue points toward the nucleosome, suggesting that it might contribute a nucleosome contact. The loss of this contact might then specifically reduce methylation of nucleosomal substrates. S304 is placed at the pseudoknot of the SET domain structure, which connects different parts of the protein directly with the active center. Our data suggest that this residue could be relevant to activate the enzyme after binding to nucleosomes. The increased activity of S304Y on peptide substrates might indicate that S304 is involved in an inhibition of SUV420H1 activity prior to nucleosome binding. This result would place SUV420H1 in line with several chromatin-modifying enzymes [48,49] and DNA methyltransferases [50], which are regulated by allosteric effects and autoinhibition.

In summary, from a mechanistic point of view, our data permit important insights into the control and regulation of SUV420H1. We provide novel and strong evidence for the role of nucleosomal contacts in the regulation of SUV420H1 activity, and we identified residues involved in allosteric regulation. Moreover, the central importance of the contact between H4 residue D24 and K258 of SUV420H1 for peptide binding and methylation is directly supported by the results of our study.

From a pathophysiological perspective, it is striking to note that seven of the eight SUV420H1 cancer mutations studied here led to a reduction in catalytic activity, which may suggest that SUV420H1 activity has a tumor suppressive function. This finding could be explained by the role of H4K20me2/3 in DNA repair [22–26], because loss or reduction of SUV420H1 activity could contribute to a mutator phenotype, which is a general characteristic of cancer cells. In agreement with this model, it has been shown that an SUV420H inhibitor induced a DNA repair phenotype in human cells [25]. This observation is also in agreement with the observation that loss of histone H4K20 trimethylation is correlated with poor prognosis and increased invasive activity in breast cancer [32].

However, despite the enrichment of mutations disrupting the catalytic activity of SUV420H1 in tumors, which we documented here, genetic data show that deletions of the SUV420H1 gene and mutations leading to the loss of the SUV420H1 protein are rare in cancers. In contrast, the gene is often amplified and overexpressed. This apparent contradiction may suggest that SUV420H1 has multiple and divergent roles in tumorigenesis and non-catalytic functions of SUV420H1 could have an oncogenic role. These could be related to the involvement of the protein in important signaling complexes including histone acetyltransferases, BRD1 and GR. This model could explain the occurrence of contradicting genetic changes in SUV420H1, which lead to inactivation of the enzyme but not loss of the protein.

Acknowledgements

This work has been supported by the DFG (JE 252/10; A.J.) and a bilateral exchange of academics support grant of the DAAD (H.E.). We thankfully acknowledge the generous gift of research materials from colleagues. Dr. Gunnar Schotta proved different SUV420H1 expression constructs and the SUV420H dko cells. The Widom 601 plasmid was a gift of Dr. Felix Müller-Planitz, and histone expression constructs were provided by Dr. Robert Schneider.

Author Contributions: A.J., S.K. and S.W. devised the project. A.B. conducted most of biochemical experiment, with support from M.S. and S. W. H.E. was involved in cloning the mutants and initial purifications. T.S. was involved in the nucleosome reconstitution. A.J., S.K. and S.W. provided technical advice and supervised the research. P.R. devised and supervised the construction of stable SUV420H1 expression cell lines. A.B. and A.J. wrote the manuscript draft and prepared the figures. All authors contributed to data interpretation and discussion, read and approved the final manuscript.

Appendix A. Supplementary data

Supplementary data to this article can be found online at https://doi.org/10.1016/j.jmb.2019.06.021.

Received 26 March 2019;
Received in revised form 19 June 2019;
Accepted 21 June 2019
Available online 27 June 2019

Keywords:
histone methylation;
protein lysine methylation;
H4K20 methylation;
protein lysine methyltransferase;
somatic cancer mutations

Abbreviations used:
AdoMet, *S*-adenosyl-L-methionine; GR, glucocorticoid receptor; CD, circular dichroism; MEF, mouse embryonic fibroblast; PKMT, protein lysine methyltransferase; dko, double knock-out; BRD1, Bromodomain-containing protein 1.

References

[1] C.D. Allis, T. Jenuwein, The molecular hallmarks of epigenetic control, Nat Rev Genet 17 (2016) 487–500.
[2] A.A. Soshnev, S.Z. Josefowicz, C.D. Allis, Greater than the sum of parts: complexity of the dynamic epigenome, Mol. Cell 69 (2018) 533.
[3] A. Jeltsch, J. Broche, P. Bashtrykov, Molecular processes connecting DNA methylation patterns with DNA methyltransferases and histone modifications in mammalian genomes, Genes (Basel) 9 (2018).
[4] H. Gowher, A. Jeltsch, Mammalian DNA methyltransferases: new discoveries and open questions, Biochem. Soc. Trans. 46 (2018) 1191–1202.
[5] C. Martin, Y. Zhang, The diverse functions of histone lysine methylation, Nat Rev Mol Cell Biol 6 (2005) 838–849.
[6] E.L. Greer, Y. Shi, Histone methylation: a dynamic mark in health, disease and inheritance, Nat Rev Genet 13 (2012) 343–357.
[7] M.L. Suva, N. Riggi, B.E. Bernstein, Epigenetic reprogramming in cancer, Science 339 (2013) 1567–1570.
[8] S. Kudithipudi, A. Jeltsch, Role of somatic cancer mutations in human protein lysine methyltransferases, Biochim. Biophys. Acta 1846 (2014) 366–379.
[9] S. Jorgensen, G. Schotta, C.S. Sorensen, Histone H4 lysine 20 methylation: key player in epigenetic regulation of genomic integrity, Nucleic Acids Res. 41 (2013) 2797–2806.
[10] L. Balakrishnan, A. Gefroh, B. Milavetz, Histone H4 lysine 20 mono- and tri-methylation define distinct biological processes in SV40 minichromosomes, Cell Cycle 9 (2010) 1320–1332.
[11] X. Cheng, Structure and function of DNA methyltransferases, Annu. Rev. Biophys. Biomol. Struct. 24 (1995) 293–318.
[12] P.A. Del Rizzo, R.C. Trievel, Molecular basis for substrate recognition by lysine methyltransferases and demethylases, Biochim. Biophys. Acta 1839 (2014) 1404–1415.
[13] G. Schotta, M. Lachner, K. Sarma, A. Ebert, R. Sengupta, G. Reuter, D. Reinberg, T. Jenuwein, A silencing pathway to induce H3-K9 and H4-K20 trimethylation at constitutive heterochromatin, Genes Dev. 18 (2004) 1251–1262.
[14] J.D. Stender, G. Pascual, W. Liu, M.U. Kaikkonen, K. Do, N. J. Spann, M. Boutros, N. Perrimon, M.G. Rosenfeld, C.K. Glass, Control of proinflammatory gene programs by regulated trimethylation and demethylation of histone H4K20, Mol. Cell 48 (2012) 28–38.
[15] H. Wu, A. Siarheyeva, H. Zeng, R. Lam, A. Dong, X.H. Wu, Y. Li, M. Schapira, M. Vedadi, J. Min, Crystal structures of the human histone H4K20 methyltransferases SUV420H1 and SUV420H2, FEBS Lett. 587 (2013) 3859–3868.
[16] S.M. Southall, N.B. Cronin, J.R. Wilson, A novel route to product specificity in the Suv4-20 family of histone H4K20 methyltransferases, Nucleic Acids Res. 42 (2014) 661–671.
[17] S. Weirich, S. Kudithipudi, A. Jeltsch, Specificity of the SUV4-20H1 and SUV4-20H2 protein lysine methyltransferases and methylation of novel substrates, J. Mol. Biol. 428 (2016) 2344–2358.
[18] H. Oda, I. Okamoto, N. Murphy, J. Chu, S.M. Price, M.M. Shen, M.E. Torres-Padilla, E. Heard, D. Reinberg, Monomethylation of histone H4-lysine 20 is involved in chromosome structure and stability and is essential for mouse development, Mol. Cell. Biol. 29 (2009) 2278–2295.
[19] K. Luger, A.W. Mader, R.K. Richmond, D.F. Sargent, T.J. Richmond, Crystal structure of the nucleosome core particle at 2.8 Å resolution, Nature 389 (1997) 251–260.
[20] S. Gonzalo, M. Garcia-Cao, M.F. Fraga, G. Schotta, A.H. Peters, S.E. Cotter, R. Eguia, D.C. Dean, M. Esteller, T. Jenuwein, M.A. Blasco, Role of the RB1 family in stabilizing histone methylation at constitutive heterochromatin, Nat. Cell Biol. 7 (2005) 420–428.
[21] G. Schotta, R. Sengupta, S. Kubicek, S. Malin, M. Kauer, E. Callen, A. Celeste, M. Pagani, S. Opravil, I.A. De La Rosa-Velazquez, A. Espejo, M.T. Bedford, A. Nussenzweig, M. Busslinger, T. Jenuwein, A chromatin-wide transition to H4K20 monomethylation impairs genome integrity and programmed DNA rearrangements in the mouse, Genes Dev. 22 (2008) 2048–2061.
[22] M.V. Botuyan, J. Lee, I.M. Ward, J.E. Kim, J.R. Thompson, J. Chen, G. Mer, Structural basis for the methylation state-specific recognition of histone H4-K20 by 53BP1 and Crb2 in DNA repair, Cell 127 (2006) 1361–1373.
[23] K.Y. Hsiao, C.A. Mizzen, Histone H4 deacetylation facilitates 53BP1 DNA damage signaling and double-strand break repair, J. Mol. Cell Biol. 5 (2013) 157–165.
[24] C.T. Tuzon, T. Spektor, X. Kong, L.M. Congdon, S. Wu, G. Schotta, K. Yokomori, J.C. Rice, Concerted activities of distinct H4K20 methyltransferases at DNA double-strand breaks regulate 53BP1 nucleation and NHEJ-directed repair, Cell Rep. 8 (2014) 430–438.
[25] K.D. Bromberg, T.R. Mitchell, A.K. Upadhyay, C.G. Jakob, M. A. Jhala, K.M. Comess, L.M. Lasko, C. Li, C.T. Tuzon, Y. Dai, F. Li, M.S. Eram, A. Nuber, N.B. Soni, V. Manaves, M.A. Algire, R.F. Sweis, M. Torrent, G. Schotta, C. Sun, M.R. Michaelides, A.R. Shoemaker, C.H. Arrowsmith, P.J. Brown, V. Santhakumar, A. Martin, J.C. Rice, G.G. Chiang, M. Vedadi, D. Barsyte-Lovejoy, W.N. Pappano, The SUV4-20 inhibitor A-196 verifies a role for epigenetics in genomic integrity, Nat. Chem. Biol. 13 (2017) 317–324.
[26] J. Lukas, C. Lukas, J. Bartek, More than just a focus: the chromatin response to DNA damage and its role in genome integrity maintenance, Nat. Cell Biol. 13 (2011) 1161–1169.
[27] L.W. Tsang, N. Hu, D.A. Underhill, Comparative analyses of SUV420H1 isoforms and SUV420H2 reveal differences in their cellular localization and effects on myogenic differentiation, PLoS One 5 (2010), e14447.
[28] Y. Wang, G. Rank, Z. Li, Y. Wang, J. Ju, A. Nuber, Y. Wu, M. Liu, M. Nie, F. Huang, L. Cerruti, C. Ma, R. Tan, G. Schotta, S.M. Jane, C.K. Zeng, Q. Zhao, Epsilon-globin expression is regulated by SUV4-20h1, Haematologica 101 (2016) e168–e172.
[29] T. Fryland, J.H. Christensen, J. Pallesen, M. Mattheisen, J. Palmfeldt, M. Bak, J. Grove, D. Demontis, J. Blechingberg, H.

S. Ooi, M. Nyegaard, M.E. Hauberg, N. Tommerup, N. Gregersen, O. Mors, T.J. Corydon, A.L. Nielsen, A.D. Borglum, Identification of the BRD1 interaction network and its impact on mental disorder risk, Genome Med 8 (2016) 53.
[30] Y. Chinenov, M.A. Sacta, A.R. Cruz, I. Rogatsky, GRIP1-associated SET-domain methyltransferase in glucocorticoid receptor target gene expression, Proc. Natl. Acad. Sci. U. S. A. 105 (2008) 20185–20190.
[31] Y. Jiang, Y. Han, S. Petrovski, K. Owzar, D.B. Goldstein, A.S. Allen, Incorporating functional information in tests of excess de novo mutational load, Am. J. Hum. Genet. 97 (2015) 272–283.
[32] Y. Yokoyama, A. Matsumoto, M. Hieda, Y. Shinchi, E. Ogihara, M. Hamada, Y. Nishioka, H. Kimura, K. Yoshidome, M. Tsujimoto, N. Matsuura, Loss of histone H4K20 trimethylation predicts poor prognosis in breast cancer and is associated with invasive activity, Breast Cancer Res. 16 (2014) R66.
[33] T. Vougiouklakis, K. Sone, V. Saloura, H.S. Cho, T. Suzuki, N. Dohmae, H. Alachkar, Y. Nakamura, R. Hamamoto, SUV420H1 enhances the phosphorylation and transcription of ERK1 in cancer cells, Oncotarget 6 (2015) 43162–43171.
[34] C. Plass, S.M. Pfister, A.M. Lindroth, O. Bogatyrova, R. Claus, P. Lichter, Mutations in regulators of the epigenome and their connections to global chromatin patterns in cancer, Nat Rev Genet 14 (2013) 765–780.
[35] A.P. Feinberg, M.A. Koldobskiy, A. Gondor, Epigenetic modulators, modifiers and mediators in cancer aetiology and progression, Nat Rev Genet 17 (2016) 284–299.
[36] S. Weirich, A. Jeltsch, Mutations in histone lysine methyltransferases and demethylases, in: P. Boffetta, P. Hainaut (Eds.), *Encyclopedia of Cancer*, 3rd ed, vol. 2, Elsevier, Academic Press 2019, pp. 538–550.
[37] A. Jeltsch, T. Lanio, Site-directed mutagenesis by polymerase chain reaction, Methods Mol. Biol. 182 (2002) 85–94.
[38] C. Fellmann, T. Hoffmann, V. Sridhar, B. Hopfgartner, M. Muhar, M. Roth, D.Y. Lai, I.A. Barbosa, J.S. Kwon, Y. Guan, N. Sinha, J. Zuber, An optimized microRNA backbone for effective single-copy RNAi, Cell Rep. 5 (2013) 1704–1713.
[39] S. Kasinathan, G.A. Orsi, G.E. Zentner, K. Ahmad, S. Henikoff, High-resolution mapping of transcription factor binding sites on native chromatin, Nat. Methods 11 (2014) 203–209.
[40] H. Klinker, C. Haas, N. Harrer, P.B. Becker, F. Mueller-Planitz, Rapid purification of recombinant histones, PLoS One 9 (2014), e104029.
[41] K. Luger, T.J. Rechsteiner, T.J. Richmond, Preparation of nucleosome core particle from recombinant histones, Methods Enzymol. 304 (1999) 3–19.
[42] P.T. Lowary, J. Widom, New DNA sequence rules for high affinity binding to histone octamer and sequence-directed nucleosome positioning, J. Mol. Biol. 276 (1998) 19–42.
[43] R. Benetti, S. Gonzalo, I. Jaco, G. Schotta, P. Klatt, T. Jenuwein, M.A. Blasco, Suv4-20h deficiency results in telomere elongation and derepression of telomere recombination, J. Cell Biol. 178 (2007) 925–936.
[44] D. Shechter, H.L. Dormann, C.D. Allis, S.B. Hake, Extraction, purification and analysis of histones, Nat. Protoc. 2 (2007) 1445–1457.
[45] S.A. Forbes, D. Beare, H. Boutselakis, S. Bamford, N. Bindal, J. Tate, C.G. Cole, S. Ward, E. Dawson, L. Ponting, R. Stefancsik, B. Harsha, C.Y. Kok, M. Jia, H. Jubb, Z. Sondka, S. Thompson, T. De, P.J. Campbell, COSMIC: somatic cancer genetics at high-resolution, Nucleic Acids Res. 45 (2017) D777–D783.
[46] Gao, J., Aksoy, B. A., Dogrusoz, U., Dresdner, G., Gross, B., Sumer, S. O., Sun, Y., Jacobsen, A., Sinha, R., Larsson, E., Cerami, E., Sander, C. & Schultz, N. (2013). Integrative analysis of complex cancer genomics and clinical profiles using the cBioPortal. *Sci Signal* **6**, pl1.
[47] E. Cerami, J. Gao, U. Dogrusoz, B.E. Gross, S.O. Sumer, B. A. Aksoy, A. Jacobsen, C.J. Byrne, M.L. Heuer, E. Larsson, Y. Antipin, B. Reva, A.P. Goldberg, C. Sander, N. Schultz, The cBio cancer genomics portal: an open platform for exploring multidimensional cancer genomics data, Cancer Discov 2 (2012) 401–404.
[48] B.E. Zucconi, P.A. Cole, Allosteric regulation of epigenetic modifying enzymes, Curr. Opin. Chem. Biol. 39 (2017) 109–115.
[49] J.A. Kim, M. Kwon, J. Kim, Allosteric regulation of chromatin-modifying enzymes, Biochemistry 58 (2019) 15–23.
[50] A. Jeltsch, R.Z. Jurkowska, Allosteric control of mammalian DNA methyltransferases—a new regulatory paradigm, Nucleic Acids Res. 44 (2016) 8556–8575.